# Regulation of Cholinergic Phenotype in Developing Neurons

**Xinhuai Liu**[1,*], **Ion R. Popescu**[1,*], **Janna V. Denisova**[2], **Rachael L. Neve**[3], **Roderick A. Corriveau**[4], **Andrei B. Belousov**[1,2]

[1]Department of Cell and Molecular Biology, Tulane University, New Orleans, Louisiana

[2]Department of Molecular and Integrative Physiology, University of Kansas Medical Center, Kansas City, Kansas

[3]McLean Hospital, Harvard Medical School, Belmont, Massachusetts

[4]Coriell Institute for Medical Research, Camden, New Jersey

## Abstract

Specification of neurotransmitter phenotype is critical for neural circuit development and is influenced by intrinsic and extrinsic factors. Recent findings in rat hypothalamus in vitro suggest the role of neurotransmitter glutamate in the regulation of cholinergic phenotype. Here we extended our previous studies on the mechanisms of glutamate-dependent regulation of cholinergic phenotypic properties in hypothalamic neurons. Using immunocytochemistry, electrophysiology, and calcium imaging, we demonstrate that hypothalamic expression of choline acetyltransferase (the cholinergic marker) and responsiveness of neurons to acetylcholine (ACh) receptor agonists increase during chronic administration of an *N*-methyl-D-aspartate receptor (NMDAR) blocker, MK-801, in developing rats in vivo and genetic and pharmacological inactivation of NMDARs in mouse and rat developing neuronal cultures. In hypothalamic cultures, an inactivation of NMDA receptors also induces ACh-dependent synaptic activity, as do inactivations of PKA, ERK/MAPK, CREB, and NF-$\kappa$B, which are known to be regulated by NMDA receptors. Interestingly, the increase in cholinergic properties in developing neurons that is induced by NMDAR blockade is prevented by the blockade of ACh receptors, suggesting that function of ACh receptor is required for the cholinergic up-regulation. Using dual recording of monosynaptic excitatory postsynaptic currents, we further demonstrate that chronic inactivation of ionotropic glutamate receptors induces the cholinergic phenotype in a subset of glutamatergic neurons. The phenotypic switch is partial as ACh and glutamate are coreleased. The results suggest that developing neurons may not only coexpress multiple transmitter phenotypes, but can also change the phenotypes following changes in signaling in neuronal circuits.

DISCLOSURE

There is no potential conflict of interests for any of the authors.

## INTRODUCTION

The choice of neurotransmitter phenotype is a fundamental event in fate specification of a developing neuron that plays an important role in the formation of neuronal circuits. Multiple mechanisms and signaling pathways are involved in neurotransmitter specification in various regions of the nervous system. These mechanisms share common principles, but also have differences. One common principle is $Ca^{2+}$-dependence of neurotransmitter specification. Changes in the activity of $Ca^{2+}$ pathways affect the expression of noradrenaline and acetylcholine (ACh) in sympathetic neurons in rodents (Walicke and Patterson 1981); dopamine in rat sensory ganglia (Brosenitsch et al. 1998); $\gamma$-aminobutyric acid (GABA), ACh, glutamate, and glycine in *Xenopus* spinal neurons (Spitzer et al. 2004); and ACh in rat hypothalamus and cerebellum (Belousov et al. 2001, 2002) [e.g., the expression of cholinergic markers consistently increases in different regions of the nervous system during decrease in the activity of $Ca^{2+}$-regulated signaling pathways (Belousov et al. 2002; Spitzer et al. 2004; Walicke and Patterson 1981)]. On the other hand, the same neurotransmitter is regulated by various target-derived diffusible molecules (e.g., cholinergic properties can be regulated by BMP-9, NT3, NGF, LIF, CNTF, and other neurotrophic factors) (Landis 1996; Lopez-Coviella et al. 2000). Furthermore, specification by intrinsic transcription factors has been demonstrated for ACh, noradrenaline, serotonin, dopamine, glutamate, and GABA (Cheng et al. 2005; Goridis and Rohrer 2002; Mori et al. 2004) [e.g., the expression of ACh in chick spinal cord interneurons is induced by L3/Lhx8 (Mori et al. 2004)].

Our recent studies in rat hypothalamic cultures in vitro suggest the regulation of the expression of one neurotransmitter (ACh) by another neurotransmitter (glutamate) during development (Belousov et al. 2001, 2002). The studies demonstrate that a long-term decrease in glutamate synaptic transmission increases the number of cholinergic neurons, the expression of nicotinic and muscarinic ACh receptors (AChRs), and induces ACh-dependent excitatory synaptic activity (Belousov et al. 2001, 2002). The data suggest the importance of *N*-methyl-D-aspartate receptors (NMDARs) and $Ca^{2+}$-dependent signaling pathways in the cholinergic up-regulation and imply that cholinergic properties are induced in postmitotic noncholinergic neurons (Belousov et al. 2002). Here we show that chronic administration of an NMDAR blocker in rats in vivo and knockout of NMDAR subunit 1 (NMDAR1) in mice also induce cholinergic phenotypic properties in hypothalamic neurons. We demonstrate the contribution of protein kinase A (PKA), extracellular signal-regulated kinase/ mitogenactivated protein kinase (ERK/MAPK), $Ca^{2+}$/cAMP response element binding protein (CREB), and nuclear factor-kappa B (NF-$\kappa$B) in cholinergic phenotype specification. We also demonstrate that a chronic decrease in excitatory glutamate transmission induces the cholinergic phenotype in a fraction of glutamatergic neurons and that both neurotransmitters are coreleased in these cells.

## METHODS

### MK-801 treatment

Sprague–Dawley rat male pups received daily subcutaneous injections of the NMDAR blocker dizocilpine (MK-801; dissolved in sterile saline): 0.5 mg/kg in 15 $\mu$l on postnatal

days 1–5 (P1–P5), 0.75 mg/kg in 40 $\mu$l on P6–P10, 1 mg/kg in 75 $\mu$l on P11–P22, and 1.5 mg/kg in 100 $\mu$l on P23–P32. The control group received saline injections (volumes as just cited). In some experiments, the treatment (saline or MK-801) was stopped on P32 and the animals were maintained and sacrificed on P55–P60.

### Slice preparation and electrophysiology

Rats were anesthetized with nembutal (70 mg/kg), sacrificed, and coronal 400-$\mu$m-thick hypothalamic slices were cut as described (Arumugam et al. 2005). Slices were prepared (at 2–4°C) and kept (at 20–22°C) in artificial cerebrospinal fluid (ACSF) containing (in mM): 124 NaCl, 3.0 KCl, 2.0 CaCl$_2$, 2.0 MgCl$_2$, 1.23 NaH$_2$PO$_4$, 26 NaHCO$_3$, and 10 glucose (aerated, pH 7.4, 325 mosm). The pipette solution contained (in mM): 145 KMeSO$_4$, 10 HEPES, 2 MgCl$_2$, 0.1 CaCl$_2$, 1.1 EGTA, 2 Na-ATP, and 0.3 Na-GTP (pH 7.2, 310 mosm, 3–6 M$\Omega$ electrode resistance). Magnocellular neurons were identified in the hypothalamic paraventricular nucleus (PVN) and the supraoptic nucleus (SON) as described (Arumugam et al. 2005). Whole cell current-clamp and continuous voltage-clamp recordings were performed using a Mutliclamp 7A amplifier and pCLAMP9 software (Molecular Devises). Cells were held at −70 mV (voltage-clamp) or −60 mV (current-clamp), i.e., close to the resting membrane potential (usually −60 to −70 mV). A flow pipe perfusion system was used for the cell perfusion (Belousov et al. 2001). Responses of neurons to carbachol were tested in ACSF containing bicuculline (20 $\mu$M; GABA$_A$-receptor antagonist), 6-cyano-7-nitroquinoxaline-2,3-dione (CNQX, 10 $\mu$M; a non-NMDAR antagonist), and MK-801 (10 $\mu$M) to prevent the secondary activation or inactivation of neurons by, respectively, endogenous glutamate and GABA. A neuron was considered as responding to carbachol if, during carbachol administration, voltage (in current-clamp) and current (in voltage-clamp) changed by, respectively, >2 mV and >5 pA from the initial background level. Data were analyzed using Igor Pro (WaveMetrics) and InStat (GraphPad) software.

### Culture preparation and treatment

Neuronal cultures were prepared from embryonic day 18–19 (E18–E19) hypothalamus obtained from pregnant Sprague–Dawley rats. At this stage of embryonic development, the hypothalamus is relatively well formed and is easily distinguished from the surrounding forebrain and brain-stem regions. The hypothalamus was identified on the ventral aspect of the brain with the exterior border delineated by the optic chiasm and the posterior border delineated by the infundibular stalk. Pregnant rats were anesthetized with nembutal, the embryos were removed, the hypothalamus was dissected, and the tissue (combined from several embryos) was processed for cell culture preparation as described (Belousov et al. 2001). Neurons were plated on glass coverslips and raised in glutamate- and glutamine-free minimal essential medium (Invitrogen) with supplements (Belousov et al. 2001). The culture medium was changed twice a week. Cell survival was determined using a toxicity assay (Live/Dead Kit; Invitrogen) as described (Belousov et al. 2001) and was not affected under the chronic treatments studied. Only CREB viral vectors induced neurodegeneration in cultures after 7–10 days; therefore cells were exposed to viral vectors for no more than 5 days [i.e., on days in vitro 30–35 (DIV30–DIV35) older cultures were used in these tests because cholinergic activity develops faster in mature cultures (Belousov et al. 2001)]. Pharmacological treatments were performed using sister cultures. Because inactivation of

non-NMDARs alone does not increase the expression of choline acetyltransferase (ChAT) and cholinergic activity in hypothalamic cultures (Belousov et al. 2002), but a combined blockade of both NMDARs and non-NMDARs has a greater effect on the cholinergic up-regulation than the blockade of only NMDARs (Belousov et al. 2002), in some experiments in the present work we used the combined blockade of NMDARs with D,L-2-amino-5-phosphonovalerate (AP5, 100 $\mu$M) and non-NMDARs with CNQX (10 $\mu$M) to get a more pronounced increase in cholinergic functions. For other treatments, the concentrations were chosen based on data from the literature and our previous studies (Arumugam et al. 2005) and, as a rule, the low range of previously reported agent concentrations were used in this study.

### Culture electrophysiology

Standard bathing solution contained: 158.5 mM NaCl, 2.5 mM KCl, 2 mM $CaCl_2$, 10 mM HEPES, 10 mM glucose, 1 $\mu$M glycine, 10 nM pituitary adenylate cyclase activating polypeptide-38 (PACAP-38, which enhances ACh-mediated spontaneous activity), and 50 $\mu$M bicuculline (pH 7.3; 325 mosm; 20–22°C). The pipette solution was the same as that for slice recordings. Discontinuous voltage-clamp whole cell recordings were made at −60 mV holding potential using one or two Axoclamp-2B amplifiers and pCLAMP7 software. In experiments with the recording of miniature excitatory postsynaptic currents (mEPSCs), each cell was recorded for 60 or 120 s. After that, the cells were held for an additional 5–10 min to see whether the very low frequency mEPSCs could be found. Focal extracellular stimulation was obtained using a Grass S48 stimulator and a double-barrel pipette designed for single-cell stimulation. The pipette (filled with bath solution) was positioned within 10–15 m of a presynaptic candidate. The monosynaptic connection between the recorded cell and the stimulated cell (i.e., presynaptic candidate) was tested by inducing an inward current (square voltage step of 0.2 ms) in the presynaptic cell. If a connection was not found, the pipette was moved to test other candidates until a monosynaptic connection was established. Monosynaptic connections were also studied using dual whole cell recordings where an inward current was generated in one cell, causing reliable, short latency (<5 ms) postsynaptic current in another cell (see Supplemental Fig. S1).[1] After completion of all tests, the presynaptic cell was ablated with an electrode to confirm that the postsynaptic response disappeared and was not an artifact. The probability of finding a monosynaptic connection was higher in recordings with focal stimulation (4/17) than in dual recordings (14/253) because the focal stimulation pipette could be moved until the connection was found, whereas the stable dual recording could be obtained in only one pair at a time.

In AP5 + CNQX–treated cultures spontaneous excitatory postsynaptic currents (EPSCs), mEPSC, focal, and dual recordings were made in the presence of AP5 + CNQX (250/25 $\mu$M). In control and AP5 + CNQX–treated cultures eserine (50 $\mu$M; an inhibitor of acetylcholine esterase) was in all media in mEPSC, focal, and dual recordings. In mEPSC recordings, all tests were done in the presence of tetrodotoxin (TTX, 2 $\mu$M; a voltage-gated sodium channel blocker). A flow pipe perfusion system was used for the cell perfusion

---

[1]The online version of this article contains supplemental data.

(Belousov et al. 2001). Data were analyzed using InStat software. Decay time of EPSCs was calculated using Mini Analysis (Synaptosoft); the values reported are the half-width.

### NMDAR1 knockout mice

NMDAR1 knockout animals and their wild-type littermates were generated by timed breeding of NMDAR1 heterozygous adults using an established NMDAR1 knockout line (Li et al. 1994). Plug day was designated E0.5. Because NMDAR1 knockout mice die 12–24 h after birth due to respiratory distress (they are born alive and appear healthy for ~10 h), it was necessary to prepare neuronal cultures from embryonic mice to study changes in cholinergic properties. At E18.5, dams were anesthetized, embryos were removed, and hypothalamic cultures were prepared as described earlier for rats. In mouse cultures, however, each plating (coverslip) contained the hypothalamic material from a single embryo. All embryos (and the corresponding coverslips) were randomly numbered and genotyped by polymerase chain reaction as described (Arumugam et al. 2005). After the experiments were finished, the results from each particular coverslip were matched with the genotyping data for the corresponding embryo. In addition in $Ca^{2+}$ imaging experiments, knockouts were verified by the absence of neuronal NMDA responses (see Supplemental Fig. S2).

### $Ca^{2+}$ imaging

Fura-2 calcium imaging was performed in cultures as described (Belousov et al. 2001). Perfusion solution contained: 137 mM NaCl, 25 mM glucose, 10 mM HEPES, 5 mM KCl, 1 mM $MgCl_2$, 3 mM $CaCl_2$, and 1 $\mu$M glycine (pH 7.4; 22°C). Calcium standards from Molecular Probes were used to calibrate the imaging system (Belousov et al. 2001). Calibrated $Ca^{2+}$ data were analyzed with Igor Pro and InStat software. No significant difference in the background $Ca^{2+}$ level was detected among neurons from various cell culture conditions (usually 45–80 nM in different cells). Culture tests with nicotine and muscarine were done in the presence of 2 $\mu$M TTX, 100 $\mu$M AP5, and 10 $\mu$M CNQX to prevent the secondary activation or inactivation of neurons. The expression of ACh-mediated $Ca^{2+}$ activity was tested in cultures during neuronal disinhibition with the $GABA_A$-receptor antagonist bicuculline (50 $\mu$M) in the presence of glutamate receptor antagonists, AP5 + CNQX [100 $\mu$M + 10 $\mu$M, which effectively suppress spontaneous glutamate-mediated activity (Belousov et al. 2001)]. A neuron was considered as responding to bicuculline if, during bicuculline application, $Ca^{2+}$ increased by >15 nM from the initial background level or intracellular $Ca^{2+}$ oscillations appeared (also 15 >nM in amplitude) and lasted for 2 min during the continued administration of bicuculline. Part of this bicuculline-mediated activity is cholinergic (Belousov et al. 2001) and part is not (Belousov et al. 2004). In the present study, to identify the cholinergic contribution to the bicuculline-mediated $Ca^{2+}$ activity, AChR antagonists atropine and mecamylamine were used (10 $\mu$M each or 100 $\mu$M each, applied jointly). Previous experiments demonstrated (Belousov et al. 2001) that, at these concentrations, atropine and mecamylamine exert only specific, receptor-mediated effects, and do not affect isolated glutamate-dependent activity. A neuron was considered as exhibiting cholinergic activity (cholinergic response) if the amplitude of bicuculline-mediated $Ca^{2+}$ increase was reduced in this neuron >50% by AChR antagonists. The amplitude of $Ca^{2+}$ increase was measured in neuronal cell bodies either at the peak of response (in cells with sustained $Ca^{2+}$ increase) or by averaging peaks of several oscillations

(in oscillating cells). For other pharmacological agents (e.g., nicotine, muscarine, etc.), the same criteria as for bicuculline were used to consider a neuron as responsive to the agent. In some experiments, NMDA-containing, but $Mg^{2+}$-free, solution was used to confirm that cells were healthy and responsive. Each test was done blindly on three to six coverslips from three independent culture preparations.

### Immunohistochemistry

After deep anesthesia with nembutal, animals were perfused transcardially with 25 ml ACSF followed by perfusion with 50 ml of phosphate-buffered saline (PBS, 0.01 M, pH 7.4) containing 4% paraformaldehyde. The brain was removed and trimmed by cutting off the tissue rostral to the optic chiasm, caudal to the hypothalamus, 3–4 mm lateral to the midline on both sides of the brain, and above the basal ganglia (i.e., by cutting below the corpus callosum). The trimmed block was placed overnight in 4% paraformaldehyde in PBS and then for 2 days at 4°C in 30% sucrose dissolved in PBS. The tissue was embedded using OCT (Sakura Finetek, Torrance, CA), frozen, and 40-$\mu$m-thick coronal sections were cut using a cryostat. The double staining was performed using the following protocol. Slices were rinsed in PBS, incubated for 6 h at 4°C in goat anti-ChAT antibody (Chemicon, Cat. #AB144P; 1:200 dilution), then rinsed and incubated for 12 h at 4°C in goat anti-ChAT antibody (as earlier) plus mouse anti-NeuN antibody (Chemicon, Cat. #MAB377; 1:200), then rinsed again and incubated for 2 h at 22°C with secondary antibodies (FITC-conjugated donkey anti-goat IgG, Jackson ImmunoResearch, Cat. #705–095-003, 1:100, and Texas Red–conjugated rabbit antimouse IgG, Jackson ImmunoResearch, Cat. #315–075-045, 1:100). Next, the sections were rinsed, mounted on slides, air-dried, and coverslipped with Vectashield-hardset (Vector Laboratories). Stained sections were visualized with an Olympus fluorescent microscope and appropriate filters. Images were taken using a Hamamatsu digital camera and analyzed off-line using OpenLab software (Improvision). To take images, the light settings were used at which most of the field's background was very dark. In each particular slice, the same settings were applied to take photomicrographs from different areas of the slice. Any cell for which staining was brighter than the background was considered as ChAT-positive. To determine the hypothalamic areas that express ChAT-positive neurons, >50 coronal sections from both groups of animals between bregma −0.26 and −2.30 mm (Paxinos and Watson 1998) were inspected. The expression of ChAT-positive cells was observed along the rostrocaudal axis in the area dorsolateral to the SON. Therefore for the purpose of comparison between the two animal groups, the analysis was done between bregma −1.30 and −1.42 mm. Further, the number of ChAT-positive and NeuN-positive cells was calculated in the sections inside two $330 \times 330$-$\mu$m square fields, one in each hemisphere (the location of one counting field is schematically illustrated in Supplemental Fig. S3). The analysis was done in 35 sections from 14 saline-treated and 45 sections from 17 MK-801–treated animals. The sections were randomly numbered and analyzed blindly as described (Arumugam et al. 2005). Negative controls included staining for the secondary antibody without preincubation with the primary antibody.

### Drugs, reagents, and viruses

All drugs were obtained from Sigma-RBI unless otherwise specified. CREB and NF-$\kappa$B oligodeoxynucleotides (ODNs) were obtained from Oligo's Etc. (Wilsonville, OR). CREB

ODN (5′-TGG TCA TCT AGT CAC CGG TG-3′) is reverse and complementary to base pairs 27–46 of rat CREB1 mRNA and is phosphorothioate modified (substitution of a sulfur for an oxygen) between each of the last three bases on both the 5′ and 3′ ends. This modification slows the degradation of ODN by exonucleases. CREB ODN decreases CREB by blocking CREB translation (Guzowski and McGaugh 1997). Double-stranded NF-$\kappa$B decoy ODNs were generated as described previously (Cao et al. 2004) using equimolar amounts of single-stranded sense (5′-AGT TGA GGG GAC TTT CCC AGGC-3′) and antisense (3′-TCA ACT CCC CTG AAA GGG TCCG-5′) phosphorothioate-modified ODNs containing both the specific NF-$\kappa$B1 (GGGAC) and RelA (TTCC) binding sites. The sequence of the scrambled (nonsense) CREB ODN was: 5′-GTC TGC AGT CGA TCT ACG GT-3′. The sequences of the scrambled NF-$\kappa$B ODNs were: 5′-TTG CCG TAC CTG ACT TAG CC-3′ and 3′-AAC GGC ATG GAC TGA ATC GG-5′. Active and scrambled ODNs were administered to the cultures daily in the following concentrations: CREB, 2 $\mu$mol/l; NF-$\kappa$B, 10 $\mu$mol/l. Herpes simplex virus CREB vector (HSV-CREB) and dominant-negative mutant form of CREB (HSV-mCREB) were prepared as described (Carlezon Jr et al. 1998). HSV-mCREB, which contains a single point mutation Ala for Ser at residue 133, cannot be phosphorylated but still binds to the $Ca^{2+}$/cAMP response element, thus preventing the binding of active CREB molecules (Carlezon Jr et al. 1998). The estimated titer of recombinant viral stocks was $1 \times 10^8$ infectious units/ml. Viruses were added to cultures once (0.25 $\mu$l stock/ml) on DIV30 and the cultures were tested on DIV35. The CREB constructs that were used in the present study (CREB ODN, HSV-CREB, and HSV-mCREB) effectively change CREB expression in hypothalamic neuronal cultures (Arumugam et al. 2005). The double-stranded NF-$\kappa$B decoy ODN is identical to that used by a number of other laboratories and its suppressing effect on NF-$\kappa$B activity was also extensively characterized (Cao et al. 2004).

## Statistical analysis

Data were analyzed using the ANOVA followed by the post hoc Tukey test, Fisher's exact probability test or the Student's *t*-test (two-tailed paired when possible), and InStat software. Fisher's exact probability test was chosen over the chi-square test to analyze proportional data because the cell count in some experiments was less than five. In all graphs/figures, data are reported as mean ± SE unless otherwise specified.

# RESULTS

## Inactivation of NMDARs in rats in vivo

Our previous work demonstrated that chronic NMDAR blockade causes up-regulation of cholinergic markers in rat hypothalamic cultures (Belousov et al. 2001, 2002). In the present studies we first tested whether the cholinergic properties are increased in hypothalamic neurons in developing rats in vivo following chronic administration of the NMDAR blocker MK-801. Double immunostaining for a neuron-specific nuclear protein NeuN (that demonstrates neuronal distribution; Fig. 1, A and C) and ChAT (ACh biosynthetic enzyme; Fig. 1, B and D) was performed in the hypothalamus from two groups of P32 rats: controls and those treated chronically (P1–P32) with MK-801. ChAT-positive neurons were present along the rostrocaudal axis in the area dorsolateral to the SON (Fig. 1, B and D), but were

sparse or absent in other hypothalamic regions. ChAT-positive terminals were spread in most of the hypothalamic nuclei, including the PVN and SON (not shown). In the area dorsolateral to the SON, the number of NeuN-positive cells was not different between the two groups (Fig. 1E), indicating that chronic treatment with MK-801 did not change the number of neurons. However, the number of ChAT-positive cells was higher in MK-801–treated animals than that in controls (Fig. 1F).

Electrophysiology was performed on acute slices of the SON and the PVN, the regions that receive cholinergic projections from the area dorsolateral to the SON (Mason et al. 1983). Whole cell current-clamp and voltage-clamp recordings were made from 167 magnocellular neurons in slices obtained from three groups of control animals (P20–P21, P31–P32, and P55–P60) and three groups of MK-801–treated animals (same age; P1–P32 treatment). Neuronal sensitivity to a general muscarinic and nicotinic AChR agonist, carbachol (200 $\mu$M), was tested. The cholinergic response was confirmed by coadministration of the nicotinic and/or muscarinic AChR antagonists, mecamylamine (20 $\mu$M) and atropine (10 $\mu$M). The responsiveness of the neurons to carbachol was higher in P20–P21 and P31–P32 in MK-801–treated animals than in controls, but was not different between the two groups at P55–P60, i.e., 23–28 days after ceasing the MK-801 administration (Fig. 2A). Of 41 neurons that were carbachol-sensitive, 38 (92.7%) responded by depolarization (current-clamp; Fig. 2B) and/or inward current (voltage-clamp; not shown) and 3 (7.3%) responded by hyperpolarization (Fig. 2C) and/or outward current (not shown). Of the group of 38 neurons that responded by depolarization and/or inward current, the amplitude of depolarization was analyzed in 24 cells (i.e., all of those tested in current-clamp). Although there was no significant change in the amplitude of depolarization from P20–P21 to P31–P32 within experimental groups (i.e., among MK-801–treated, or among controls), the depolarization amplitude was higher in MK-801–treated animals than that in controls [9.7 ± 0.4 mV ($n =$ 18) vs. 7.6 ± 1.1 mV ($n = 6$); $P = 0.017$, Student's $t$-test; data for P20–P22 and P31–P32 are combined]. The low probability of hyperpolarizing responses precluded analyses of differences in hyperpolarization amplitude as well as the low responsiveness in P55–P60 animals did not allow a comparison of this group with others. The results indicate that chronic administration of the NMDAR blocker during development in vivo increases both the number of cholinergic neurons in the area dorsolateral to the SON and the cholinergic responsiveness in the SON and the PVN.

### NMDAR1 knockout mice

Mice that lack NMDAR1, the essential subunit for NMDAR function, were used to complement the pharmacological approach that was used in developing rats. Because NMDAR1 knockout mice die 12–24 h after birth due to respiratory distress, the expression of ChAT, cholinergic responses, and ACh-dependent activity were studied in hypothalamic neuronal cultures prepared from NMDAR1 knockout mice and their wild-type littermates. Four culture groups were tested on DIV18: wild-type control; wild-type chronically treated (DIV4–DIV18) with AP5 (100 $\mu$M; NMDAR antagonist) plus CNQX (10 $\mu$M; non-NMDAR antagonist); wild-type chronically treated with AP5 alone; and NMDAR1 knockout. In all cases chronic depletion of NMDAR function (AP5 + CNQX–treated, AP5-treated, and NMDAR1 knockout) resulted in increased numbers of ChAT-positive neurons versus

controls (Fig. 3, A–D; Table 1). Responsiveness of neurons to nicotine (50 $\mu$M, nicotinic AChR agonist) and muscarine (50 $\mu$M, muscarinic AChR agonist), as measured by $Ca^{2+}$ imaging, also was higher in the three experimental groups than that in controls (Fig. 4, A–D; Table 2). Furthermore, acute blockade of $GABA_A$ receptors (with bicuculline, 50 $\mu$M) in the presence of AP5 + CNQX (100/10 $\mu$M) revealed ACh-mediated $Ca^{2+}$ transients in many neurons in AP5 + CNQX–treated, AP5-treated, and NMDAR1 knockout cultures, but not in the control cultures (Fig. 4, E–H; Table 3). The results suggest that genetic deletion of NMDAR1 increases the cholinergic properties in developing neurons in cultures and this increase is comparable to that in wild-type cultures subjected to the pharmacological inactivation of NMDARs.

### Role of AChRs in the regulation of cholinergic properties

Using the approaches described earlier, we tested whether cholinergic properties develop in neurons during chronic (DIV4–DIV18) inactivation of ionotropic glutamate receptors when the activity of AChRs is also suppressed. Three groups of rat hypothalamic cultures were tested: nontreated (control); treated with AP5 + CNQX (100/10 $\mu$M); and treated with AP5 + CNQX plus mecamylamine and atropine (100 $\mu$M each). These AChR antagonists completely prevented the increase in the expression of ChAT, cholinergic responsiveness in neurons, and ACh-dependent activity (Tables 1–3). This suggests that the function of AChRs is required for the up-regulation of cholinergic properties due to chronic glutamate receptor blockade.

### NMDAR antagonists

We compared the effects of two NMDAR antagonists, AP5 (a competitive NMDAR antagonist) and MK-801 (an NMDAR channel blocker; which we also used in in vivo experiments), on the expression of ChAT and ACh-dependent activity in rat hypothalamic cultures. AP5 and MK-801 were chronically added to cultures (DIV4–DIV18) in concentrations of, respectively, 100 and 20 $\mu$M (these concentrations completely block the NMDAR-mediated neuronal responses; not shown). The cultures were tested on DIV18 using ChAT immunostaining and $Ca^{2+}$ imaging approaches as illustrated in Figs. 3 and 4, E–H. The number of ChAT-positive neurons and the expression of cholinergic activity increased in both experimental groups of cultures, although the increase was higher in AP5-treated than in MK-801–treated cultures (Tables 1 and 3; see DISCUSSION for the interpretation of these results).

### Mechanisms of cholinergic regulation

Hypothalamic neuronal cultures respond to chronic inactivation of NMDARs, L-type voltage-gated $Ca^{2+}$ channels, $Ca^{2+}$/calmodulin-dependent protein kinases II/IV (CaMKII/IV), or protein kinase C (PKC) by developing cholinergic activity and increasing the number of ChAT-positive neurons (Belousov et al. 2002). This suggests the $Ca^{2+}$-dependent regulation of cholinergic properties. In the nervous system, PKA, ERK/MAPK, CREB, and NF-$\kappa$B are also regulated by NMDARs and $Ca^{2+}$-dependent signaling pathways (Bernal-Mizrachi et al. 2002; Greenberg and Ziff 2001; Guan et al. 2005; Lilienbaum and Israel 2003; Lonze and Ginty 2002). Therefore we tested whether chronic inactivation of PKA, ERK/MAPK, CREB, and NF-$\kappa$B also induce cholinergic activity in rat hypothalamic

neuronal cultures. To avoid neurotoxic effects of some of the reagents (see METHODS), treatments were performed in cultures on DIV30–DIV35. To determine the expression of ACh-dependent activity, a $Ca^{2+}$ imaging approach was used as illustrated for mouse cultures in Fig. 4, E–H.

Chronic inactivation of PKA (with H89, 1 $\mu$M) or ERK/MAPK (with PD98059, 30 $\mu$M) both induced ACh-dependent activity in cultures (Table 3). Similarly, overexpression of a mutant form of CREB (with HSV-mCREB) and treatment of cells with CREB ODN (2 $\mu$mol/l), NF-$\kappa$B decoy ODN (10 $\mu$mol/l), or rapamycin (100 nM; inhibitor of NF-$\kappa$B) all induced ACh-mediated activity in neurons. Accordingly, overexpression of CREB (with HSV-CREB) blocked induction of ACh-mediated activity by chronic treatment with AP5 + CNQX. Moreover, combined treatment of cultures with CREB ODN and NF-$\kappa$B ODN had a greater effect in the induction of cholinergic activity (26.1% of neurons) than each treatment separately (20.1 and 12.6%, respectively). Neither CREB nor NF-$\kappa$B scrambled ODNs (2 and 10 $\mu$mol/l, respectively) had an effect. The results indicate that PKA, ERK/MAPK, CREB, and NF-$\kappa$B pathways are involved in the regulation of cholinergic activity in developing hypothalamic neurons.

### ACh-dependent postsynaptic activity

To address the identity of the neurons that develop cholinergic phenotype following glutamate receptor blockade, and whether the resulting neurotransmitter phenotype is pure or mixed, we first studied the expression of postsynaptic excitatory activity in nontreated (control) rat hypothalamic cultures and cultures chronically treated (for 14–17 days, starting on DIV4) with AP5 + CNQX (100/10 $\mu$M). Tests were done on DIV18–DIV21 using whole cell recording. Spontaneous EPSCs were detected in all neurons tested in control cultures ($n$ = 10; Fig. 5Aa1). The EPSCs were completely suppressed by acute application of AP5 + CNQX (100/10 $\mu$M; Fig. 5Aa2) and thus were glutamatergic; therefore no excitatory activity other than glutamatergic is expressed in the control cultures.

In contrast, in cultures that were chronically treated with AP5 + CNQX, 7 of 24 neurons (29.2%) demonstrated spontaneous EPSCs when tested in the presence of equal or higher concentrations of these glutamate receptor antagonists (250/25 $\mu$M; Fig. 5Bb1). These EPSCs were suppressed by the nicotinic AChR antagonists d-tubocurarine (d-TC, 40 $\mu$M) and/or mecamylamine (100 $\mu$M) (Fig. 5Bb2), indicating that they are cholinergic. Subsequent removal of AP5 + CNQX while the AChR antagonists remained present revealed spontaneous glutamate-mediated EPSCs in the same chronically treated neurons ($n$ = 7 of 7; Fig. 5Bb3) as well as in other neurons ($n$ = 17 of 24; 70.8%) that did not show cholinergic EPSCs in the presence of AP5 + CNQX (not shown). In AP5 + CNQX–treated cultures, the isolated spontaneous glutamate-mediated EPSCs had a higher frequency, amplitude, and shorter decay time than the isolated cholinergic EPSCs (Fig. 5, C–F).

We also tested whether mEPSCs, which do not require action potentials (AP) and are caused by neurotransmitter release from single synaptic vesicles (Del Castillo and Katz 1954), are expressed in the two groups of cultures. All mEPSCs were analyzed in the presence of TTX (2 $\mu$M), a voltage-gated sodium channel antagonist that blocks APs. In control cultures no mEPSCs were detected in the presence of AP5 + CNQX, and most cells ($n$ = 9 of 11,

81.8%) demonstrated glutamatergic mEPSCs after the AP5 + CNQX mixture was removed (not shown). In cultures chronically treated with AP5 + CNQX, no mEPSCs were detected in the presence of AP5 + CNQX ($n = 64$ neurons; Fig. 5Gg1), indicating an absence of cholinergic mEPSCs. As expected, the removal of AP5 + CNQX revealed the glutamatergic mEPSCs ($n = 36$ of 42 neurons, 85.7%; Fig. 5Gg2).

### Monosynaptic EPSCs

Since in AP5 + CNQX–treated cultures, cholinergic EPSCs are detected in neurons in which glutamatergic EPSCs are also detected (the preceding data), and cholinergic properties are induced in postmitotic noncholinergic neurons (Belousov et al. 2002), we set out to determine whether ACh and glutamate are released from the same neurons. We first used a single-cell focal stimulation approach. Monosynaptic contacts were established in whole cell patch-clamp recordings from neurons by stimulating single presynaptic neurons with an extracellular electrode designed for single-cell stimulation. A AP5 + CNQX (250/25 $\mu$M) mixture was maintained in the cultures during recording. Short latency (2–5 ms) focal monosynaptic EPSCs were detected in 4 of 17 tested neurons and were partially ($n = 2$; Fig. 6A) or completely ($n = 2$; Fig. 6B) suppressed by the AChR antagonists d-TC (40 $\mu$M) or mecamylamine plus atropine (100 $\mu$M each). All neurons with ACh-mediated EPSCs, when examined, also displayed larger, faster decaying monosynaptic (2–5 ms) glutamatergic EPSCs ($n = 4$; Fig. 6, A–D). In addition, glutamatergic EPSCs were established in 4 of 10 neurons that did not display cholinergic EPSCs (not shown).

As a second approach for analyzing monosynaptic EPSCs in AP5 + CNQX–treated cultures, we used dual whole cell recording with stimulation of one neuron and recording from another neuron. AP5 + CNQX (250/25 $\mu$M) was maintained in the cultures during recording. Monosynaptic (2–5 ms) EPSCs were detected in 14 of 253 neuronal pairs and were pharmacologically tested in 6 of them. The EPSCs were partially ($n = 5$; Fig. 6E) or completely ($n = 1$; Fig. 6F) suppressed by d-TC (40 $\mu$M) or mecamylamine plus atropine (100 $\mu$M each). In each case removing AP5 + CNQX in the presence of AChR antagonists unmasked larger, faster decaying monosynaptic (2–5 ms) glutamatergic EPSCs ($n = 6$; Fig. 6, E–H). Some neurons ($n = 4$ of 9) that did not demonstrate monosynaptic cholinergic EPSCs did display glutamatergic monosynaptic EPSCs after the AP5 + CNQX mixture was removed (not shown).

In control cultures, no monosynaptic EPSCs were observed when AP5 + CNQX was present in the media ($n = 26$). However, 9 of 10 (focal stimulation) and 5 of 16 (dual recording) neurons demonstrated glutamate-mediated monosynaptic EPSCs after removal of AP5 + CNQX (not shown).

## DISCUSSION

### Mechanisms of glutamate-dependent cholinergic regulation

Our study demonstrates that pharmacological and genetic inactivations of NMDARs increase pre- and postsynaptic cholinergic properties in developing hypothalamic neurons both in vivo and in cell culture. This includes increases in the number of cholinergic (ChAT-

positive) neurons, responsiveness to AChR agonists, and ACh-dependent spontaneous activity. These data are in agreement with previous findings indicating that chronic administration of NMDAR antagonists in rat pups in vivo increases the catalytic activity of ChAT in some regions of the CNS (Facchinetti et al. 1993; Virgili et al. 1994). In addition, activation of glutamate receptors is known to down-regulate the expression of cholinergic activity in developing hypothalamic neurons (Belousov et al. 2001) and the activity of ChAT in the developing retina (Loureiro-Dos-Santos et al. 2001). Taken together, the data support an idea on bidirectional regulation of cholinergic phenotype by a neurotransmitter glutamate.

We also report that inactivation of ERK/MAPK, PKA, CREB, or NF-$\kappa$B increases cholinergic activity in hypothalamic neurons. Relationships involving these factors may impart this regulation and place it downstream of NMDAR function. Increased intracellular $Ca^{2+}$ caused by ion flux through NMDARs induces phosphorylation of CREB by $Ca^{2+}$-dependent protein kinases (on serine 133 and, perhaps, on other sites), in turn causing the formation of a CREB dimer that binds to a $Ca^{2+}$/cAMP response element on the promoters of CREB target genes (Greenberg and Ziff 2001; Lonze and Ginty 2002). The NF-$\kappa$B family of transcription factors is composed of members (NF-$\kappa$B1, NF-$\kappa$B2, RelA, c-Rel, and RelB) that form hetero- and homodimers that, when activated by inducers (e.g., ERK/MAPK, PKA, PKC, and CaMKII), provide cytoplasmic to nuclear signaling that regulates target genes (Bernal-Mizrachi et al. 2002; Guan et al. 2005; Lilienbaum and Israel 2003). NF-$\kappa$B and CREB binding sites are both present in the 5′ regulatory region of the mouse and rat *ChAT* genes (NCBI Genebank database). Given that NF-$\kappa$B negatively regulates ChAT promoter activity (Toliver-Kinsky et al. 2000) and that CREB activation prevents chronic glutamate receptor blockade from inducing cholinergic activity (present study), we hypothesize that genes responsible for determining pre- and postsynaptic cholinergic properties in neurons are regulated directly and negatively by NF-$\kappa$B and CREB. Moreover, based on the present and previous studies (Belousov et al. 2002), we conclude that ERK/MAPK, PKA, PKC, and CaMKII/IV act downstream of NMDARs to regulate, via NF-$\kappa$B and CREB, the cholinergic phenotype in neurons.

An interesting feature of our results is that the induction of cholinergic properties during chronic glutamate receptor blockade is prevented when the neurons are coincubated in the presence of AChR antagonists. This indicates that function of AChRs is required for cholinergic up-regulation due to the inactivation of glutamate receptors. Furthermore, one of the NMDAR channel blockers used in this study, MK-801, also is known to partially decrease the activity of nicotinic AChRs (Briggs and McKenna 1996). The antinicotinic action of MK-801 may explain the observation that AP5, which is a selective NMDAR antagonist, has a stronger effect than that of MK-801 in the induction of cholinergic properties.

During inactivation of NMDARs with MK-801, an increase in the number of ChAT-positive neurons was larger in the hypothalamus in vitro than in vivo. In vitro, the number of ChAT-positive neurons increased 7.8-fold during MK-801 treatment (from 1.8 to 14.1% per microscope field). In vivo, the increase was 1.6-fold (from 5.9 to 9.4%). This difference between the in vitro and in vivo conditions is either due to an antinicotinic effect of MK-801 (see earlier text) or due to incomplete blockade of NMDARs in vivo, or both. This latter

possibility is consistent with the previous study (Vezzani et al. 1989), indicating that MK-801 reaches maximal concentration in the rat brain within 30 min of intraperitoneal injection and subsequently decreases by 50% during the following 2 h. It is estimated that NMDAR activity in the brain tissue is reduced for a period of 4–8 h after the injection. Therefore the blockade of NMDARs in our in vivo experiments most likely was partial and lasted for (at least) several hours per day. Our previous study in rat hypothalamic cultures showed that partial blockade of glutamate receptors also induces ACh-dependent activity, but to a lesser extent than complete blockade (Belousov et al. 2001). Therefore partial inactivation of NMDARs may potentially cause the difference in the number of cholinergic neurons induced by different manipulations that decrease NMDAR function in vivo and in vitro.

Previous work from our and other laboratories revealed that, during chronic glutamate receptor blockade, cholinergic properties are increased in some regions of the CNS, including the hypothalamus and cerebellum, but not in others, such as the cortex (Belousov et al. 2001; Facchinetti et al. 1993; Virgili et al. 1994). We therefore hypothesized (Belousov et al. 2001) that glutamate-dependent regulation of the cholinergic phenotype is region specific. In the present study in which rats were chronically treated with MK-801, we found that the number of ChAT-positive neurons increases in the area dorsolateral to the SON, but not in other hypothalamic regions. In this regard, it may not be coincidence that some neurons in the area dorsolateral to the SON normally express cholinergic neurons in control conditions (Mason et al. 1983), whereas other hypothalamic regions do not express ChAT-positive neurons. In other words, the results indicate that the mechanisms of glutamate-dependent regulation of the cholinergic phenotype are region specific even within the hypothalamus. It remains to be determined whether developing neurons in the area dorsolateral to the SON express low, but undetectable, levels of ChAT, and these levels are increased by chronic glutamate receptor blockade, or whether these cells do not express ChAT at all, and expression is turned on by the blockade.

As established in the present study on acute brain slices, responsiveness of neurons to carbachol decreases to the control level 23–28 days after the withdrawal of MK-801 treatment in rats in vivo. This correlates with our previous data in hypothalamic cultures, indicating that increased cholinergic properties decrease after removal of glutamate receptor antagonists from the culture medium (Belousov et al. 2001).

In the present study we demonstrate that the NMDAR blockade increases the cholinergic properties in hypothalamic neurons both on the presynaptic side (increased number of cholinergic neurons and ACh synaptic release) and on the postsynaptic side (increased sensitivity to AChR agonists, suggesting an increased expression of AChRs). However, the data suggest that up-regulation of cholinergic properties on presynaptic and postsynaptic levels is a unified process. We propose that an increase in the presynaptic synthesis and release of ACh during development dictates the necessity of a corresponding up-regulation of postsynaptic muscarinic and nicotinic AChRs. Similarly, the absence of AChR activity prevents an increase in the presynaptic ACh synthesis and release, as evident from the experiments with the combined chronic administration of glutamate and AChR antagonists. In this respect, the cholinergic activity that is revealed in $Ca^{2+}$ imaging experiments with use

of the bicuculline test reflects the cholinergic increase on both presynaptic (ACh release) and postsynaptic (AChR expression) sides.

### Induction of cholinergic phenotype in glutamatergic neurons

We also report the novel finding that, following chronic NMDAR blockade in hypothalamic cell cultures, ACh is released from a subset of glutamate-secreting neurons. These data suggest that during a long-term decrease in NMDAR function in developing neurons: *1*) the cholinergic phenotype is induced in some glutamatergic neurons, *2*) the switch in phenotype is partial (as demonstrated by neurotransmitter corelease), and *3*) some glutamatergic neurons maintain their phenotype and do not develop the cholinergic properties.

Although in AP5 + CNQX–treated cultures, almost one third of neurons displayed spontaneous cholinergic EPSCs, none exhibited cholinergic mEPSCs. On the other hand, in the same cultures, glutamatergic currents were found in many neurons in both spontaneous EPSC (100%) and mEPSC (86%) recordings. As noted earlier, spontaneous EPSCs are AP-dependent, but mEPSCs are not (Del Castillo and Katz 1954). Moreover, the frequency of APs is not different between neurons in control and AP5 + CNQX–treated hypothalamic cultures (Belousov et al. 2001). Therefore one possibility is that in hypothalamic neurons an AP-independent vesicular release of ACh is minimal and most (if not all) synaptic ACh release is AP-dependent; glutamate, however, is released in both an AP-dependent and an AP-independent manner. An alternative explanation for the absence of ACh-mediated mEPSCs in AP5 + CNQX–treated hypothalamic neurons, however, could be the following: ACh is released in an AP-independent manner, although ACh molecules are quickly degraded in the synaptic cleft by acetylcholine esterase and do not reach the postsynaptic receptors; only massive release of ACh-containing vesicles during AP causes the postsynaptic EPSC. Our data correlate with the observation by Jo and Schlichter (1999) who established the corelease of ATP and GABA from spinal neurons, but demonstrated only spontaneous GABA-mediated postsynaptic currents and not spontaneous ATP-mediated postsynaptic events.

In control cultures, no spontaneous cholinergic EPSCs were detected in the presence of AP5 + CNQX. One reason for this could be that the cholinergic EPSCs are expressed by the control neurons, but spontaneous circuit-generated spike activity is so low in the absence of glutamatergic drive that there are not enough APs to trigger ACh-dependent EPSCs. The absence of evoked cholinergic EPSCs in similar conditions (i.e., in the presence of acute AP5 + CNQX) argues that spontaneous cholinergic activity indeed is absent in the control hypothalamic cultures.

The monosynaptic data suggest a corelease of ACh and glutamate from the same neurons; however, because the coincidence of ACh- and glutamate-dependent mEPSCs have not been established, we cannot conclude whether the two neurotransmitters are being released from the same or different synaptic vesicles. Future studies with the use of electron microscopy and double ACh and glutamate immunostaining will further clarify this issue.

### Is there a third neurotransmitter?

In a few cases coapplication of ACh and glutamate receptor antagonists failed to fully block monosynaptic EPSCs (Fig. 6). Because the concentrations of AP5 + CNQX in these tests were 150% higher than those during the chronic culture incubation (250/25 $\mu$M vs. 100/10 $\mu$M), the unblocked EPSC was unlikely due to activation by glutamate of hypersensitized ionotropic glutamate receptors. Given the fast dynamics of the unblocked EPSCs, it also was unlikely due to glutamate acting on metabotropic glutamate receptors. This suggests that another (the third) neurotransmitter contributes to these EPSCs.

The presence of noncholinergic and nonglutamatergic activity is also evident in $Ca^{2+}$ imaging recordings from some neurons in AP5 + CNQX–treated cultures where the bicuculline-induced activity is not suppressed by ACh and glutamate receptor antagonists (Table 3). Previous work (Belousov et al. 2004) indicates that a number of neurotransmitter receptors contribute to the generation of such a noncholinergic/nonglutamatergic activity. This includes P2-purinoreceptors, histamine receptors, and adrenoreceptors. Therefore it is possible that ATP, histamine, and/or noradrenaline are coexpressed with ACh and glutamate and are responsible for a nonblocked monosynaptic EPSC. In control hypothalamic neurons, no excitatory neurotransmitters are presumably coreleased with glutamate because all glutamatergic monosynaptic EPSCs are completely eliminated by the blockade of ionotropic glutamate receptors.

### Functional implications

Multiple reports suggest corelease and/or colocalization of ACh and glutamate in developing or mature neurons. This has been demonstrated in rat and squirrel monkey mesopontine tegmentum (Clarke et al. 1997; Lavoie and Parent 1994); rat cerebellum, striatum, and septum (Boulland et al. 2004; Danik et al. 2005); rat and mouse motor neurons (Koyuncuoglu et al. 1998; Nishimaru et al. 2005; Waerhaug and Ottersen 1993); and *Xenopus* spinal cord (Li et al. 2004). Developmental switches in neurotransmitter phenotypes have also been documented. Neurons in the developing rat central auditory pathways first corelease GABA, glycine, and glutamate, then become GABA and glycine coreleasing, and finally take on a predominantly glycinergic phenotype in the adult (Gillespie et al. 2005; Nabekura et al. 2004). Rabbit starburst amacrine cells in the retina initially express both GABA and ACh, and then become purely GABAergic (Zheng et al. 2004). In the rat sympathetic nervous system, noradrenergic neurons become cholinergic, passing through a state in which the neuron secretes both noradrenaline and ACh (Potter et al. 1986).

Cholinergic markers and synaptic transmission are transiently expressed in many regions of the mammalian and avian nervous system (hypothalamus, spinal cord, retina, cerebellum, etc.) during embryonic and early postnatal development (Clos et al. 1989; Feller et al. 1996; Milner and Landmesser 1999; Zoli et al. 1995). These cholinergic properties are subsequently down-regulated at later developmental stages that coincide with the glutamatergic synapse formation and increased glutamate-dependent excitatory synaptic activity (Wong 1999). However, cholinergic properties can be induced in a number of CNS

regions after prolonged inactivation of NMDARs both in vivo and in vitro (Belousov et al. 2001, 2002; Facchinetti et al. 1993; Virgili et al. 1994; this study).

It has been speculated that down-regulation of cholinergic properties during development is due to a phenotypic switch from ACh to another transmitter (Kwong et al. 2000). Based on the present results, together with previously published data, we hypothesize that *1*) in the developing hypothalamus many neurons undergo a cholinergic to glutamatergic switch in phenotypes; *2*) maturation of fast glutamatergic transmission is in part responsible for the developmental decease of early cholinergic activity; and *3*) neurons that switch their phenotype have the potential to reexpress cholinergic properties during prolonged decrease in glutamatergic synaptic transmission. Future studies in developing hypothalamic circuits will confirm or refute this hypothesis. If confirmed, however, it is likely that only a fraction of the glutamatergic neurons found in the adult derive from the cholinergic cells, and there are additional mechanisms for glutamate phenotype specification.

## Supplementary Material

Refer to Web version on PubMed Central for supplementary material.

## Acknowledgments

## REFERENCES

Arumugam H, Liu X, Colombo PJ, Corriveau RA, Belousov AB. NMDA receptors regulate developmental gap junction uncoupling via CREB signaling. Nat Neurosci 8: 1720–1726, 2005. [PubMed: 16299502]

Belousov AB, Arumugam H, Denisova JV. Noncholinergic excitation in neurons after a chronic glutamate receptor blockade. Neuroreport 15: 113–117, 2004. [PubMed: 15106842]

Belousov AB, Hunt ND, Raju RP, Denisova JV. Calcium-dependent regulation of cholinergic cell phenotype in the hypothalamus in vitro. J Neurophysiol 88: 1352–1362, 2002. [PubMed: 12205156]

Belousov AB, O'Hara BF, Denisova JV. Acetylcholine becomes the major excitatory neurotransmitter in the hypothalamus in vitro in the absence of glutamate excitation. J Neurosci 21: 2015–2027, 2001. [PubMed: 11245685]

Bernal-Mizrachi E, Wen W, Shornick M, Permutt MA. Activation of nuclear factor-kappaB by depolarization and $Ca^{2+}$ influx in MIN6 insulinoma cells. Diabetes 51, Suppl. 3: S484–S488, 2002.

Boulland JL, Qureshi T, Seal RP, Rafiki A, Gundersen V, Bergersen LH, Fremeau RT Jr, Edwards RH, Storm-Mathisen J, Chaudhry FA. Expression of the vesicular glutamate transporters during development indicates the widespread corelease of multiple neurotransmitters. J Comp Neurol 480: 264–280, 2004. [PubMed: 15515175]

Briggs CA, McKenna DG. Effect of MK-801 at the human alpha 7 nicotinic acetylcholine receptor. Neuropharmacology 35: 407–414, 1996. [PubMed: 8793902]

Brosenitsch TA, Salgado-Commissariat D, Kunze DL, Katz DM. A role for L-type calcium channels in developmental regulation of transmitter phenotype in primary sensory neurons. J Neurosci 18: 1047–1055, 1998. [PubMed: 9437025]

Cao CC, Ding XQ, Ou ZL, Liu CF, Li P, Wang L, Zhu CF. In vivo transfection of NF-kappaB decoy oligodeoxynucleotides attenuate renal ischemia/reperfusion injury in rats. Kidney Int 65: 834–845, 2004. [PubMed: 14871403]

Carlezon WA Jr, Thome J, Olson VG, Lane-Ladd SB, Brodkin ES, Hiroi N, Duman RS, Neve RL, Nestler EJ. Regulation of cocaine reward by CREB. Science 282: 2272–2275, 1998. [PubMed: 9856954]

Cheng L, Samad OA, Xu Y, Mizuguchi R, Luo P, Shirasawa S, Goulding M, Ma Q. Lbx1 and Tlx3 are opposing switches in determining GABAergic versus glutamatergic transmitter phenotypes. Nat Neurosci 8: 1510–1515, 2005. [PubMed: 16234809]

Clarke NP, Bevan MD, Cozzari C, Hartman BK, Bolam JP. Glutamate-enriched cholinergic synaptic terminals in the entopeduncular nucleus and subthalamic nucleus of the rat. Neuroscience 81: 371–385, 1997. [PubMed: 9300428]

Clos J, Ghandour S, Eberhart R, Vincendon G, Gombos G. The cholinergic system in developing cerebellum: comparative study of normal, hypothyroid and underfed rats. Dev Neurosci 11: 188–204, 1989. [PubMed: 2766963]

Danik M, Cassoly E, Manseau F, Sotty F, Mouginot D, Williams S. Frequent coexpression of the vesicular glutamate transporter 1 and 2 genes, as well as coexpression with genes for choline acetyltransferase or glutamic acid decarboxylase in neurons of rat brain. J Neurosci Res 81: 506–521, 2005. [PubMed: 15983996]

Del Castillo J, Katz B. Quantal components of the end-plate potential. J Physiol 124: 560–573, 1954. [PubMed: 13175199]

Facchinetti F, Ciani E, Dall'Olio R, Virgili M, Contestabile A, Fonnum F. Structural, neurochemical and behavioural consequences of neonatal blockade of NMDA receptor through chronic treatment with CGP 39551 or MK-801. Brain Res Dev Brain Res 74: 219–224, 1993. [PubMed: 8104744]

Feller MB, Wellis DP, Stellwagen D, Werblin FS, Shatz CJ. Requirement for cholinergic synaptic transmission in the propagation of spontaneous retinal waves. Science 272: 1182–1187, 1996. [PubMed: 8638165]

Gillespie DC, Kim G, Kandler K. Inhibitory synapses in the developing auditory system are glutamatergic. Nat Neurosci 8: 332–338, 2005. [PubMed: 15746915]

Goridis C, Rohrer H. Specification of catecholaminergic and serotonergic neurons. Nat Rev Neurosci 3: 531–541, 2002. [PubMed: 12094209]

Greenberg ME, Ziff EB. Signal transduction in the postsynaptic neuron: activity-dependent regulation of gene expression In: Synapses, edited by Cowan MW, Sudhof TC, Stevens CF. Baltimore, MD: Johns Hopkins Univ. Press, 2001, p. 357–391.

Guan H, Hou S, Ricciardi RP. DNA binding of repressor nuclear factor-kappaB p50/p50 depends on phosphorylation of Ser337 by the protein kinase A catalytic subunit. J Biol Chem 280: 9957–9962, 2005. [PubMed: 15642694]

Guzowski JF, McGaugh JL. Antisense oligodeoxynucleotide-mediated disruption of hippocampal cAMP response element binding protein levels impairs consolidation of memory for water maze training. Proc Natl Acad Sci USA 94: 2693–2698, 1997. [PubMed: 9122258]

Jo YH, Schlichter R. Synaptic corelease of ATP and GABA in cultured spinal neurons. Nat Neurosci 2: 241–245, 1999. [PubMed: 10195216]

Koyuncuoglu H, Kara I, Gunel MA, Nurten A, Yamanturk P. N-Methyl-D-aspartate antagonists, glutamate release inhibitors, 4-aminopyridine at neuromuscular transmission. Pharmacol Res 37: 485–491, 1998. [PubMed: 9695122]

Kwong WH, Chan WY, Lee KK, Fan M, Yew DT. Neurotransmitters, neuropeptides and calcium binding proteins in developing human cerebellum: a review. Histochem J 32: 521–534, 2000. [PubMed: 11127973]

Landis SC. The development of cholinergic sympathetic neurons: a role for neuropoietic cytokines? Perspect Dev Neurobiol 4: 53–63, 1996. [PubMed: 9169919]

Lavoie B, Parent A. Pedunculopontine nucleus in the squirrel monkey: distribution of cholinergic and monoaminergic neurons in the mesopontine tegmentum with evidence for the presence of glutamate in cholinergic neurons. J Comp Neurol 344: 190–209, 1994. [PubMed: 7915726]

Li WC, Soffe SR, Roberts A. Glutamate and acetylcholine corelease at developing synapses. Proc Natl Acad Sci USA 101: 15488–15493, 2004. [PubMed: 15494439]

Li Y, Erzurumlu RS, Chen C, Jhaveri S, Tonegawa S. Whisker-related neuronal patterns fail to develop in the trigeminal brain-stem nuclei of NMDAR1 knockout mice. Cell 76: 427–437, 1994. [PubMed: 8313466]

Lilienbaum A, Israel A. From calcium to NF-kappa B signaling pathways in neurons. Mol Cell Biol 23: 2680–2698, 2003. [PubMed: 12665571]

Lonze BE, Ginty DD. Function and regulation of CREB family transcription factors in the nervous system. Neuron 35: 605–623, 2002. [PubMed: 12194863]

Lopez-Coviella I, Berse B, Krauss R, Thies RS, Blusztajn JK. Induction and maintenance of the neuronal cholinergic phenotype in the central nervous system by BMP-9. Science 289: 313–316, 2000. [PubMed: 10894782]

Loureiro-Dos-Santos NE, Reis RA, Kubrusly RC, de Almeida OM, Gardino PF, de Mello MC, de Mello FG. Inhibition of choline acetyltransferase by excitatory amino acids as a possible mechanism for cholinergic dysfunction in the central nervous system. J Neurochem 77: 1136– 1144, 2001. [PubMed: 11359879]

Mason WT, Ho YW, Eckenstein F, Hatton GI. Mapping of cholinergic neurons associated with rat supraoptic nucleus: combined immunocytochemical and histochemical identification. Brain Res Bull 11: 617–626, 1983. [PubMed: 6365254]

Milner LD, Landmesser LT. Cholinergic and GABAergic inputs drive patterned spontaneous motoneuron activity before target contact. J Neurosci 19: 3007–3022, 1999. [PubMed: 10191318]

Mori T, Yuxing Z, Takaki H, Takeuchi M, Iseki K, Hagino S, Kitanaka J, Takemura M, Misawa H, Ikawa M, Okabe M, Wanaka A. The LIM homeobox gene, L3/Lhx8, is necessary for proper development of basal forebrain cholinergic neurons. Eur J Neurosci 19: 3129–3141, 2004. [PubMed: 15217369]

Nabekura J, Katsurabayashi S, Kakazu Y, Shibata S, Matsubara A, Jinno S, Mizoguchi Y, Sasaki A, Ishibashi H. Developmental switch from GABA to glycine release in single central synaptic terminals. Nat Neurosci 7: 17–23, 2004. [PubMed: 14699415]

Nishimaru H, Restrepo CE, Ryge J, Yanagawa Y, Kiehn O. Mammalian motor neurons corelease glutamate and acetylcholine at central synapses. Proc Natl Acad Sci USA 102: 5245–5249, 2005. [PubMed: 15781854]

Paxinos G, Watson C. The Rat Brain in Stereotaxic Coordinates (4th ed). San Diego, CA: Academic Press, 1998.

Potter DD, Landis SC, Matsumoto SG, Furshpan EJ. Synaptic functions in rat sympathetic neurons in microcultures. II. Adrenergic/cholinergic dual status and plasticity. J Neurosci 6: 1080–1098, 1986. [PubMed: 3009730]

Spitzer NC, Root CM, Borodinsky LN. Orchestrating neuronal differentiation: patterns of $Ca^{2+}$ spikes specify transmitter choice. Trends Neurosci 27: 415–421, 2004. [PubMed: 15219741]

Toliver-Kinsky T, Wood T, Perez-Polo JR. Nuclear factor kappaB/p49 is a negative regulatory factor in nerve growth factor-induced choline acetyltransferase promoter activity in PC12 cells. J Neurochem 75: 2241–2251, 2000. [PubMed: 11080175]

Vezzani A, Serafini R, Stasi MA, Caccia S, Conti I, Tridico RV, Samanin R. Kinetics of MK-801 and its effect on quinolinic acidinduced seizures and neurotoxicity in rats. J Pharmacol Exp Ther 249: 278–283, 1989. [PubMed: 2540317]

Virgili M, Facchinetti F, Contestabile A. Chronic neonatal NMDA blockade results in long-term cholinergic increase in the rat spinal cord. Neuroreport 5: 2023–2025, 1994. [PubMed: 7865735]

Waerhaug O, Ottersen OP. Demonstration of glutamate-like immunoreactivity at rat neuromuscular junctions by quantitative electron microscopic immunocytochemistry. Anat Embryol (Berl) 188: 501–513, 1993. [PubMed: 7906106]

Walicke PA, Patterson PH. On the role of $Ca^{2+}$ in the transmitter choice made by cultured sympathetic neurons. J Neurosci 1: 343–350, 1981. [PubMed: 6267223]

Wong RO. Retinal waves and visual system development. Annu Rev Neurosci 22: 29–47, 1999. [PubMed: 10202531]

Zheng JJ, Lee S, Zhou ZJ. A developmental switch in the excitability and function of the starburst network in the mammalian retina. Neuron 44: 851–864, 2004. [PubMed: 15572115]

Zoli M, Le Novere N, Hill JA Jr, Changeux JP. Developmental regulation of nicotinic ACh receptor subunit mRNAs in the rat central and peripheral nervous systems. J Neurosci 15: 1912–1939, 1995. [PubMed: 7891142]
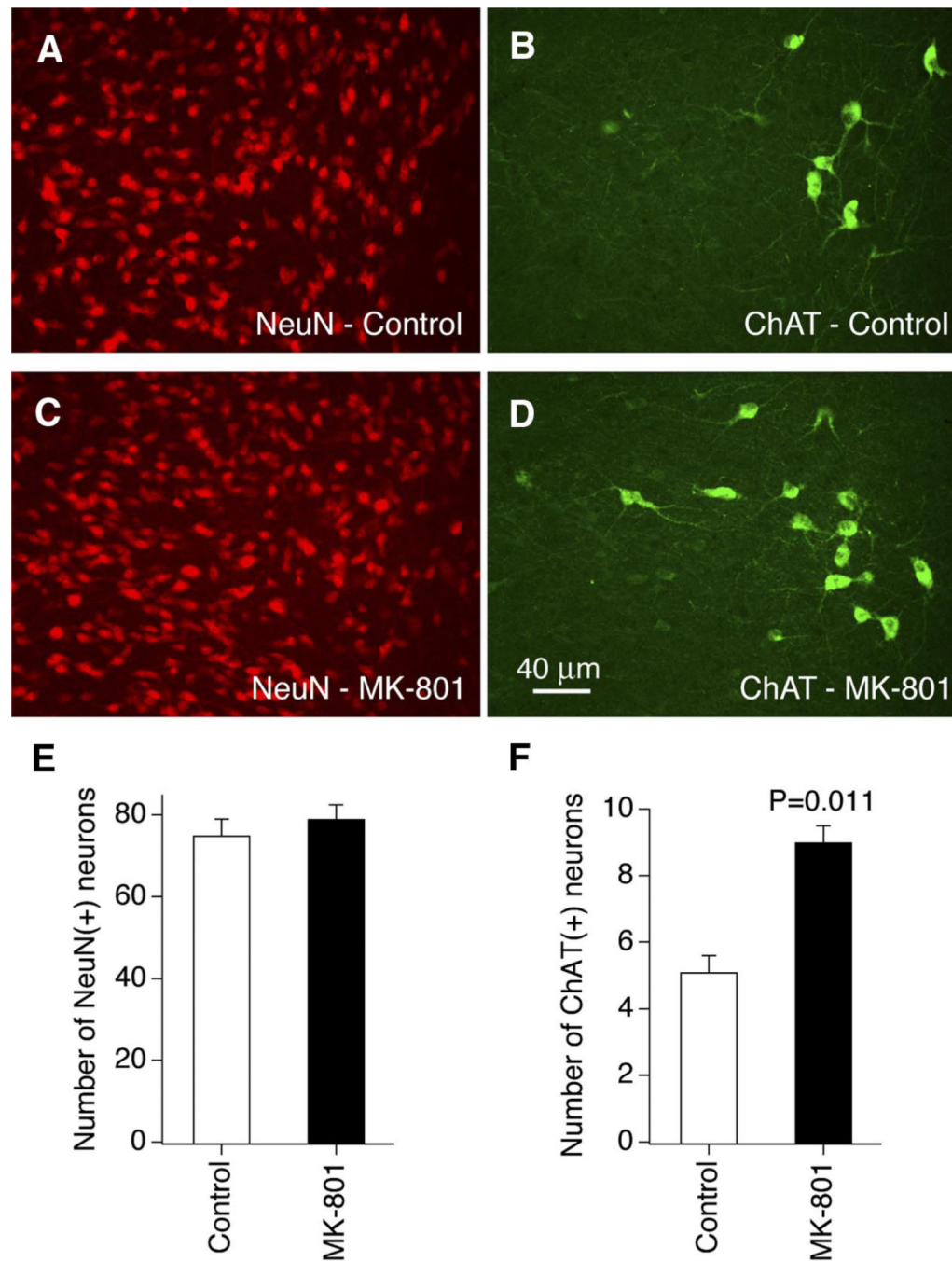
**FIG. 1.**

Chronic MK-801 treatment in vivo increases the number of cholinergic neurons in the rat hypothalamus. *A–D*: representative images of the double immunostaining for NeuN (*A, C*) and ChAT (*B, D*) in the area dorsolateral to the SON in postnatal day 32 (P32) control (*A, B*) and MK-801–treated (*C, D*) rats are shown. The pairs of images (*A* and *B*; *C* and *D*) were taken from the same fields/sections. *E* and *F*: graphs represent statistical analysis for NeuN (*E*) and ChAT (*F*) expression (Student's *t*-test; *n* = 35, control, and *n* = 45, MK-801–treated,

in both *E* and *F*). ChAT, choline acetyltransferase; MK-801, dizocilpine; NeuN, a neuron-specific nuclear protein; SON, supraoptic nucleus.
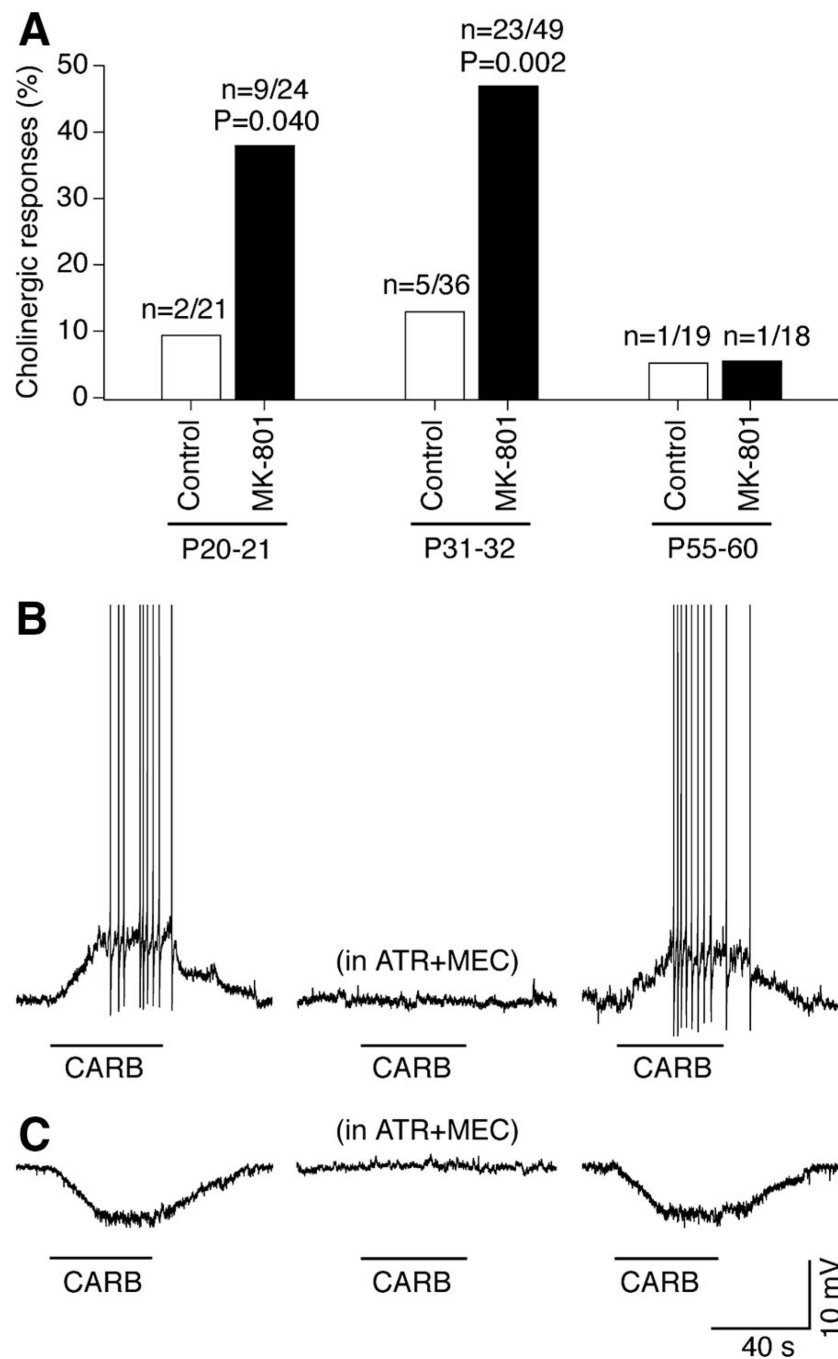
**FIG. 2.**

Chronic MK-801 treatment in vivo increases cholinergic responsiveness in the rat hypothalamus. *A*: percentage of carbachol-responsive neurons in slices [data for SON and paraventricular nucleus (PVN) are combined; excitatory and inhibitory responses are combined; $n = 167$]. The number of responding neurons of the total number of neurons and statistical significance are shown. Statistical significance was calculated relative to the corresponding control using the Fisher's exact probability test. *B* and *C*: representative traces for depolarizing (*B*) and hyperpolarizing (*C*) responses (SON; P32; MK-801–treated).

Applications of carbachol (CARB) are indicated by bars. The sequence of carbachol tests (*left* to *right*): without, in the presence, and after washout of acetylcholine receptor (AChR) antagonists (ATR + MEC, atropine + mecamylamine).
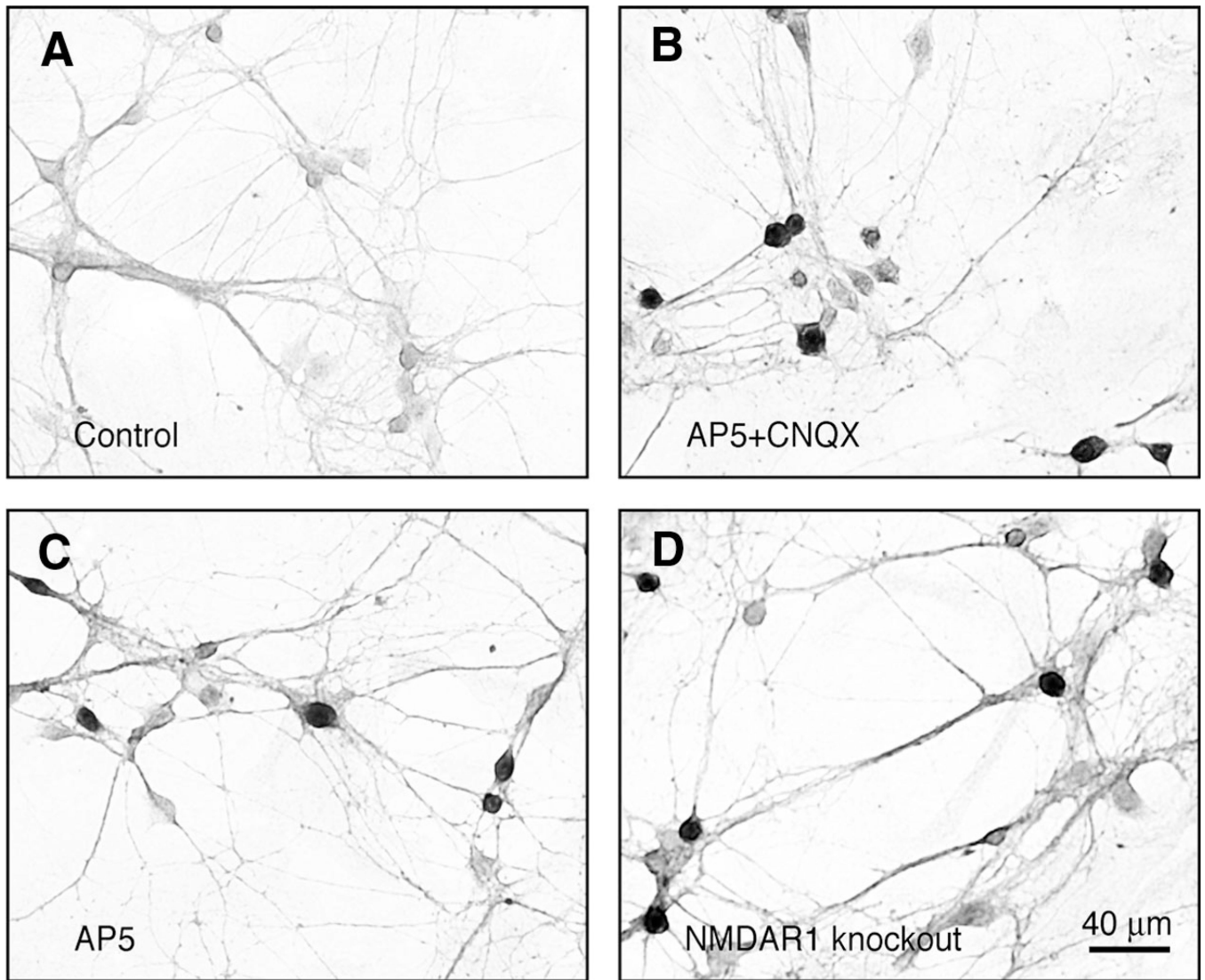
**FIG. 3.**

NMDAR1 knockout increases the number of cholinergic neurons in mouse hypothalamic cultures. Representative images are shown. *A*: most of the neurons in the control cultures were not stained for ChAT. *B–D*: ChAT-positive (dark) and ChAT-negative (light) neurons were found in AP5 + CNQX–treated (*B*), AP5-treated (*C*), and NMDAR1 knockout (*D*) cultures. AP5, D,L-2-amino-5-phosphonovalerate; CNQX, 6-cyano-7-nitroquinoxaline-2,3-dione; NMDAR1, *N*-methyl-D-aspartate receptor subunit 1.
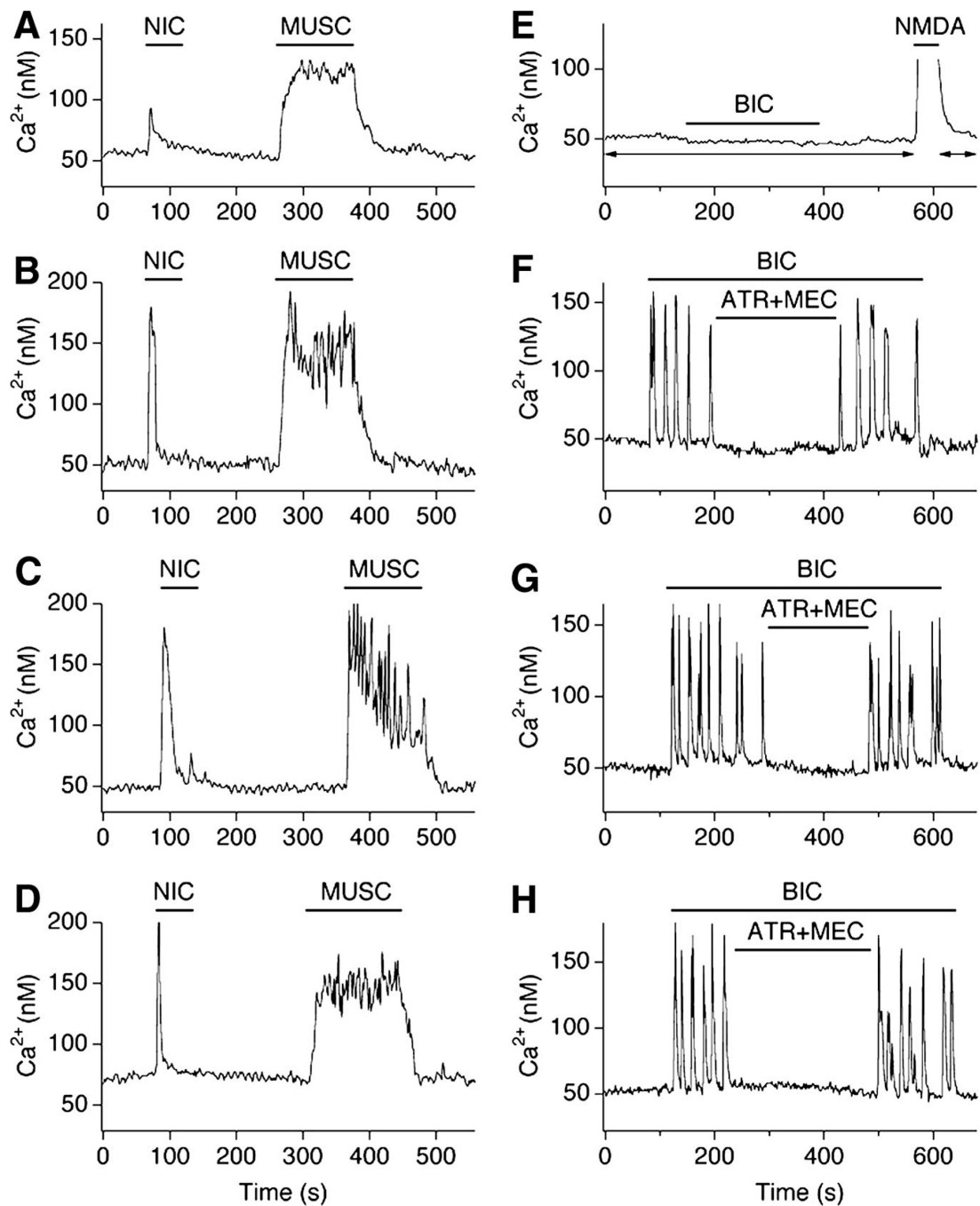
**FIG. 4.**

NMDAR1 knockout increases cholinergic responsiveness and cholinergic activity in mouse hypothalamic cultures. Representative $Ca^{2+}$ imaging recordings from neurons in control (*A, E*), AP5 + CNQX–treated (*B, F*), AP5-treated (*C, G*), and NMDAR1 knockout (*D, H*) cultures are shown. *A–D*: traces illustrate neuronal responses to nicotine (NIC) and muscarine (MUSC). In *A–D*, tetrodotoxin (TTX, 2 μM) was in all media. *E–H*: traces illustrate ACh-dependent activity. Typical control neuron did not respond to bicuculline (BIC; 50 μM) in the presence of glutamate receptor antagonists (*E*). However, neurons in the

3 experimental groups revealed $Ca^{2+}$ activity during disinhibition (*F–H*). The activity was cholinergic as was suppressed by AChR antagonists (ATR + MEC; 100 $\mu$M each). AP5 (100 $\mu$M) and CNQX (10 $\mu$M) were in all solutions in *A–H* except for the NMDA-containing (10 $\mu$M)/$Mg^{2+}$-free solution in *E* used to confirm that the cells were healthy and responsive (the presence of AP5 + CNQX in *E* is shown by arrows).
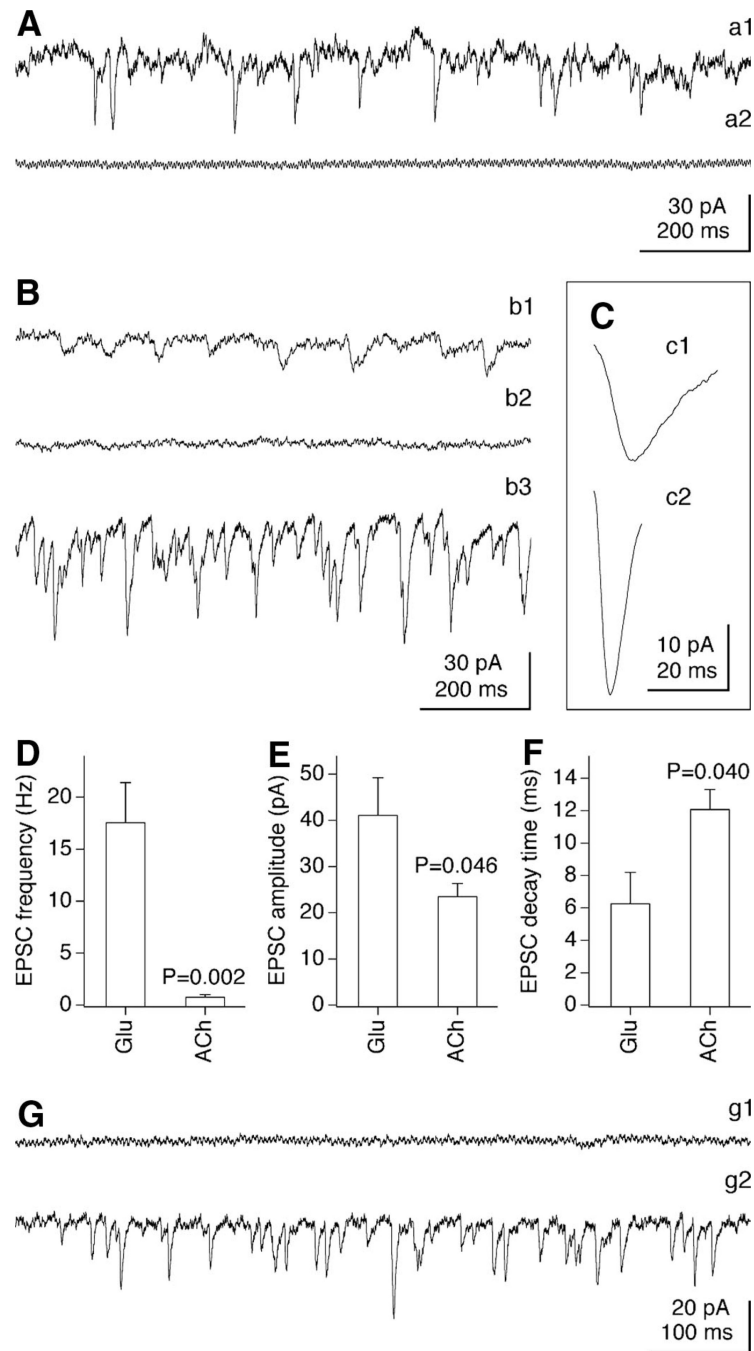
**FIG. 5.**

Glutamate- and ACh-dependent postsynaptic activity. Representative recordings from neurons in control (*A*) and AP5 + CNQX–treated (*B, C, G*) cultures demonstrate spontaneous excitatory postsynaptic currents (EPSCs, *A–C*) and miniature (m)EPSCs (*G*). *A*: spontaneous EPSCs in this control neuron (*a1*) are glutamatergic as suppressed by acute application of AP5 + CNQX (*a2*). *B*: spontaneous EPSCs in this AP5 + CNQX–treated neuron (*b1*) are cholinergic as abolished by mecamylamine plus d-TC (100 and 40 $\mu$M; *b2*). Removal of AP5 + CNQX, without washout of mecamylamine and d-TC, unmasks

glutamatergic EPSCs (*b3*). *C*: averaged (30 events) cholinergic (*c1*) and glutamatergic (*c2*) EPSCs are from the neuron shown in *B*. *D–F*: graphs represent the frequency (*D*), amplitude (*E*), and decay time (*F*) of glutamatergic (Glu) and cholinergic (ACh) spontaneous EPSCs recorded in 7 AP5 + CNQX–treated neurons. Each point represents >50 sequential EPSCs from each neuron. Statistical significance was calculated using Student's *t*-test. *G*: no mEPSCs are detected in this AP5 + CNQX–treated neuron in the presence of AP5 + CNQX (*g1*), but the removal of AP5 + CNQX unmasks glutamatergic mEPSCs (*g2*). AP5 + CNQX (100/10 $\mu$M) was in media in *a2* and AP5 + CNQX (250/25 $\mu$M) was in *b1–b2*, *c1*, and *g1*.
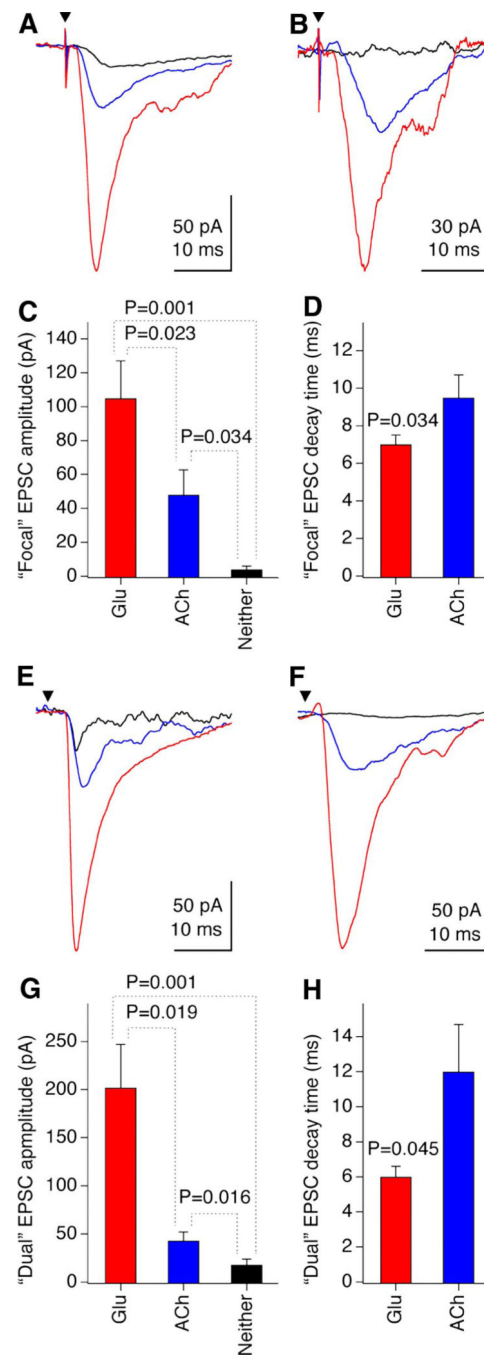
**FIG. 6.**

Corelease of ACh and glutamate from neurons in AP5 + CNQX–treated cultures. *A–D*: monosynaptic EPSCs obtained with focal stimulation (*n* = 4 neurons). *E–H*: monosynaptic EPSCs obtained with dual recording (*n* = 6 neurons). Representative recordings are illustrated in *A*, *B*, *E*, and *F*. Graphs represent the analysis (paired Student's *t*-test) for EPSC amplitude (*C*, *G*) and decay time (*D*, *H*). Red (Glu), glutamatergic EPSC isolated with AChR antagonists; blue (ACh), cholinergic EPSC isolated with glutamate receptor antagonists; black (Neither), response recorded in the presence of both ACh and glutamate

receptor antagonists (here, the decay time was not measurable). Filled triangles indicate the stimulation artifact (*A, B*) or the time of the presynaptic neuron stimulation (*E, F*). In these tests, AP5 + CNQX were used in concentrations of 250/25 $\mu$M.

**TABLE 1.**

Expression of cholinergic neurons in hypothalamic cultures

| Culture Condition | Number of Neurons p.m.f. | Percentage of ChAT-Positive Neurons p.m.f. |
|---|---|---|
| *A. Mouse (DIV4-DIV18 treatment)* | | |
| Control | $39.8 \pm 1.3$ | $1.3 \pm 0.3$ |
| AP5 + CNQX | $43.9 \pm 1.6$ | $30.8 \pm 2.4$, $*P < 0.001$ |
| AP5 | $41.3 \pm 1.4$ | $24.3 \pm 2.0$, $*P < 0.001$, $\#P < 0.05$ |
| NMDAR1 knockout | $42.4 \pm 1.2$ | $24.1 \pm 1.8$, $*P < 0.001$, $\#P < 0.05$ |
| *B. Rat (DIV4-DIV18 treatment)* | | |
| Control | $45.2 \pm 1.9$ | $1.8 \pm 0.4$ |
| AP5 + CNQX | $48.7 \pm 2.0$ | $30.7 \pm 2.3$, $*P < 0.001$ |
| AP5 + CNQX + atropine + mecamylamine | $44.7 \pm 2.9$ | $2.5 \pm 0.4$, $\#P < 0.001$ |
| AP5 | $46.1 \pm 1.9$ | $22.8 \pm 2.4$, $*P < 0.001$, $\#P < 0.05$ |
| MK-801 | $47.0 \pm 1.7$ | $14.1 \pm 2.8$, $*P < 0.001$, $\#P < 0.001$ |

Values are means ± SE. p.m.f., per microscope field. In each group, calculations were done in 10 microscope fields from three independent coverslips ($n = 30$ microscope fields; ×20 objective). Significance of differences (ANOVA with post hoc Tukey test) was calculated relative to the control (*) and AP5 + CNQX-treated (#) groups.

**TABLE 2.**

Responses of cultured hypothalamic neurons to AChR agonists

| Culture Condition | Number of Neurons Tested | Neuronal Responses to Nicotine | | Neuronal Responses to Muscarine | | Number (%) Responding to Both Agonists |
|---|---|---|---|---|---|---|
| | | Number (%) Responding | Amplitude, nM $Ca^{2+}$ | Number (%) Responding | Amplitude, nM $Ca^{2+}$ | |
| *A. Mouse (DIV4-DIV18 treatment)* | | | | | | |
| Control | 95 | 11 (11.6) | $54.5 \pm 16.5$ | 19 (20.0) | $71.8 \pm 17.4$ | 8 (8.4) |
| AP5 + CNQX | 121 | 66 (54.5) | $137.8 \pm 12.2, *P < 0.05$ | 77 (63.6) | $124.7 \pm 9.6, *P < 0.05$ | 51 (42.1) |
| AP5 | 139 | 70 (50.4) | $128.3 \pm 9.2, *P < 0.05$ | 79 (56.8) | $120.1 \pm 7.2, *P < 0.05$ | 60 (43.2) |
| NMDAR1 knockout | 163 | 79 (48.4) | $134.8 \pm 8.7, *P < 0.05$ | 96 (58.9) | $116.3 \pm 5.6, *P < 0.05$ | 64 (39.3) |
| *B. Rat (DIV4-DIV18 treatment)* | | | | | | |
| Control | 124 | 23 (18.5) | $89.9 \pm 14.9$ | 19 (15.3) | $108.0 \pm 15.2$ | 7 (5.6) |
| AP5 + CNQX | 165 | 130 (78.8) | $159.9 \pm 8.7, *P < 0.01$ | 137 (83.0) | $155.8 \pm 7.7, *P < 0.05$ | 106 (64.2) |
| AP5 + CNQX + atropine + mecamylamine | 154 | 22 (14.3) | $92.8 \pm 14.4, \#P < 0.01$ | 28 (18.2) | $94.9 \pm 7.8, \#P < 0.01$ | 3 (1.9) |

Values are means ± SE. Measurements of $Ca^{2+}$ responses were done relative to the initial background $Ca^{2+}$ levels. All neurons were tested in the presence of 2 $\mu M$ tetrodotoxin, 100 $\mu M$ AP5, and 10 $\mu M$ CNQX. Statistical significance (ANOVA with post hoc Tukey test) is relative to the control (*) and AP5 + CNQX-treated (#) groups. Values in parentheses are percentages.

**TABLE 3.**

ACh-dependent $Ca^{2+}$ activity in hypothalamic cultures grown under various cell culture conditions

| Culture Condition | Number (%) of Neurons Responding to Bicuculline | Number (%) of Neurons With the Cholinergic Response |
|---|---|---|
| *A. Mouse (DIV4-DIV18 treatment)* | | |
| Control | 0 of 176 (0) | 0 of 176 (0) |
| AP5 + CNQX | 129 of 332 (38.9) | 89 of 332 (26.8) |
| AP5 | 118 of 328 (36.0) | 82 of 328 (25.0) |
| NMDAR1 knockout | 143 of 392 (36.5) | 91 of 392 (23.2) |
| *B. Rat (DIV4-DIV18 treatment)* | | |
| Control | 0 of 143 (0) | 0 of 143 (0) |
| AP5 + CNQX | 154 of 211 (73.0) | 127 of 211 (60.2) |
| AP5 + CNQX + atropine + mecamylamine | 34 of 272 (12.5) | 0 of 272 (0) |
| AP5 | 98 of 191 (51.3) | 79 of 191 (41.4) |
| MK-801 | 55 of 183 (30.0) | 37 of 183 (20.2) |
| *C. Rat (DIV30-DIV35 treatment)* | | |
| Control | 0 of 147 (0) | 0 of 147 (0) |
| AP5 + CNQX | 46 of 109 (42.2) | 32 of 109 (29.4) |
| [AP5 + CNQX] | [95 of 213 (44.6)] | [55 of 213 (25.8)] |
| H89 | 38 of 139 (27.3) | 27 of 139 (19.4) |
| [H89] | [45 of 174 (25.9)] | [32 of 174 (18.4)] |
| PD98059 | 49 of 151 (32.5) | 34 of 151 (22.5) |
| [PD98059] | [70 of 196 (35.7)] | [35 of 196 (17.9)] |
| HSV-CREB + AP5 + CNQX | 0 of 146 (0) | 0 of 146 (0) |
| HSV-mCREB | 13 of 141 (9.2) | 7 of 141 (5.0) |
| CREB ODN | 69 of 189 (36.5) | 38 of 189 (20.1) |
| NF-$\kappa$B odn | 33 of 167 (19.8) | 21 of 167 (12.6) |
| Rapamycin | 13 of 142 (9.2) | 11 of 142(7.7) |
| CREB ODN + NF-$\kappa$B ODN | 91 of 153 (59.5) | 40 of 153 (26.1) |
| Scrambled CREB ODN | 0 of 148 (0) | 0 of 148 (0) |
| Scrambled NF-$\kappa$B ODN | 1 of 185 (0.5) | 0 of 185 (0) |

All neurons were tested in the presence of 100 $\mu$M AP5 and 10 $\mu$M CNQX in all media. The second column presents the number of neurons in which bicuculline induced intracellular $Ca^{2+}$ increases. The third column presents the number of neurons in which the bicuculline-mediated $Ca^{2+}$ increase was suppressed (by >50%) by AChR antagonists, atropine and mecamylamine (applied jointly). In most of the experiments, atropine and mecamylamine were used in the concentration of 100 $\mu$M each. In culture conditions that are demarcated by square brackets (i.e. [–]), atropine and mecamylamine instead were used in the concentration of 10 $\mu$M each. Values in parentheses are percentages.